# SENSITIVITY OF SOLAR OFF-LIMB LINE PROFILES TO ELECTRON DENSITY STRATIFICATION AND THE VELOCITY DISTRIBUTION ANISOTROPY

**N.-E. Raouafi and S. K. Solanki**

*Max-Planck-Institut für Sonnensystemforschung, 37191 Katlenburg-Lindau, Germany*

## ABSTRACT

The interpretation of observations aiming at the determination of the solar wind velocity vector and the velocity distribution in solar polar coronal holes is reviewed. In particular we investigate the effect of the electron density stratification on the profiles of the H I Ly-$\alpha$ line and the O VI and Mg X doublets formed in the solar corona. We employ an analytical 2-D model of the large scale coronal magnetic field and solar wind. We concentrate on the polar coronal holes and take into account the integration along the line of sight (LOS). We find that at distances greater than 1 $R_\odot$ from the solar surface the widths of the emitted lines of O VI and Mg X are significantly affected by the details of the adopted electron density profiles. However, H I Ly-$\alpha$ which is a pure radiative line is less affected by this effect. In particular, the densities deduced from SoHO data (Doyle et al. 1999a,b: SUMER; Kohl et al. 1998: UVCS and Lamy et al. 1997: LASCO, hereafter referred to together as DKL) result in O VI profiles whose widths and intensity ratio are relatively close to the values observed by UVCS/SoHO, although only isotropic velocity distributions are employed. Hence we expect the magnitude of the anisotropy of the velocity distribution to depend strongly on the assumed density stratification.

Key words: Line: profiles – Scattering – Sun: corona – Magnetic fields – Sun: solar wind – Sun: UV radiation.

## 1. INTRODUCTION

The solar wind acceleration and the heating of different species in the solar corona have been studied since decades. However, they still remain among the challenges of solar physics and astrophysics in general. Extreme-ultraviolet spectroscopy is a key tool to infer the plasma conditions in the solar corona. The densities, the temperatures, the bulk velocities and the velocity distributions of different species, etc., can be obtained from the intensity profiles of multiple spectral lines.

The Doppler effect provides information on the LOS velocity and can also be employed to obtain information on (microscopic and macroscopic) velocities including components perpendicular to the LOS via the so-called "Doppler dimming" of spectral lines (Hyder & Lites 1970). When moving atoms are excited by incident radiation characterized by a spectral emission profile, a Doppler shift appears between the atomic absorption profile and the incident one, so that the absorption probability of the moving atom is largest in a wing of the incident line profile. Consequently, with increasing speed of absorbing atoms relative to the gas emitting the incident profile, the absorption (or scattering) and the reemitted intensity all decrease, so that the coronal line appears dimmer.

Another application of the Doppler effect is the so-called "optical pumping", which is the excitation of the a spectral transition of a given atomic species by a neighboring line of another species. This is the case for the coronal O VI 1037.61 Å line that can be excited by the C II 1037 Å line when the solar wind speed reaches values between 100 and 250 km s$^{-1}$ (Noci et al. 1987) and by the C II 1036 Å line at speeds between 200 and 500 km s$^{-1}$, which occurs above $\sim 2.5$ $R_\odot$ from Sun center in polar coronal holes (Li et al. 1998).

One of the best known results obtained by the UltraViolet Coronagraph Spectrometer (UVCS: Kohl et al. 1995, 1997) onboard of the Solar and Heliospheric Observatory (SoHO: Domingo et al. 1995) are the very broad spectral lines emitted in polar coronal holes by heavy ions (namely O VI and Mg X) during solar activity minimum (Kohl et al. 1997, 1998; Noci et al. 1997, Habbal et al. 1997, Li et al. 1998; Cranmer et al. 1999a,b,c; etc.). For the interpretation of these profiles, it has been suggested that the velocity distributions of the heavy ions in the polar coronal holes are highly anisotropic. In addition, the heavy ions are deduced to be significantly hotter and faster than the protons. For O VI and Mg X the ratio of kinetic temperatures in the direction perpendicular and parallel to the coronal magnetic field, respectively, is found to range from 10 to 100 (Cranmer et al. 1999a,b,c). It was argued that these anisotropies are due to wave-particle interaction at the cyclotron frequencies of the different coronal species. This interpretation is supported by temperature anisotropies found at distances larger than 0.3 AU (Hundhausen 1972; Bame et al. 1975; von Steiger et al. 1995; Collier et al. 1996; Marsch 1999; etc.).

In the present paper we consider the influence of the density stratification on the profiles of spectral lines emitted in the polar coronal holes for the case of a simple model of the large-scale coronal magnetic field at the minimum of solar activity and a consistent treatment of the solar wind. We consider a set of different empirical density profiles and study the effect of the density stratification on spectral lines having different formation mechanisms (the H I Ly-$\alpha$ forms almost exclusively by resonant scattering of the solar disk radiation (the collisional contribution is negligible, Raymond et al. 1997), the O VI doublet forms by resonant scattering and by electron collisions and the

Mg X doublet at 609 and 625 Å that are formed purely by electron collisions).

## 2. LINE FORMATION IN THE CORONA

In this paper, the velocity distributions of the different species considered here are assumed to be Maxwellians with a drift velocity vector $\boldsymbol{u}$ and a width $\alpha_s$ that depends on the heliocentric distance $r$ and the considered atomic species. No anisotropy in the kinetic temperature of the scattering atoms/ions is prescribed. We also assume that the incident solar disk line profiles are Gaussians with width $\alpha_i$ (except for Ly-$\alpha$, for which a more complex shape is employed). For more details, see Raouafi & Solanki (2004).

In an optically thin medium, such as the solar corona, the intensity $\mathcal{I}(\nu, r)$ emitted at the frequency $\nu$ and at a given location on the LOS, $Z$, characterized by the heliocentric distance $r$ is generally the sum of two components: a collisional contribution $\mathcal{I}_{\rm col}(\nu, r, Z)$ and a radiative one $\mathcal{I}_{\rm rad}(\nu, r, Z)$. The spectral profiles of the collisional and radiative components are, respectively, given by

$$\exp\left[-\left(\frac{v_Z - u_Z}{\alpha_s}\right)^2\right] \quad \text{and} \quad \exp\left[-\left(\frac{v_Z - u_Z + \alpha_{si}\, n_Z\, \boldsymbol{u}\cdot\boldsymbol{n}}{[\alpha_{si}(\alpha_i^2 + \alpha_s^2(1-n_Z^2))]^{1/2}}\right)^2\right], \tag{1}$$

where $\alpha_{si} = \alpha_s^2/(\alpha_i^2 + \alpha_s^2)$ and $v_Z = c\,(\nu - \nu_0)/\nu_0$, $\nu_0$ is the rest frequency of the line. $n_Z$ is the LOS component of a unitary vector $\boldsymbol{n}$ along a radiation beam coming from an elementary area on the solar disk characterized by a solid angle $\Omega$ (see Fig. 1 in Raouafi & Solanki 2004).

According to Eq. (1), at any location along the LOS the emitted collisional and radiative profiles are both Gaussians. However, the Doppler shifts of the two components are different. The shift of the collisional component is exactly equal to the LOS macroscopic speed $u_Z$ of the scattering atoms/ions. The Doppler shift of the radiative component is generally smaller than $u_Z$ and cannot exceed a limit value that depends on the different parameters given in Eq. (1). Consequently, the LOS integrated collisional profile is wider than the radiative one. This is in addition to the fact that the radiative component is also affected by the Doppler dimming effect, which is a function of the outflow speed of the scattering atoms/ions, while the collisional component is not.

## 3. ATMOSPHERIC PARAMETERS

A realistic interpretation of the observed spectral profiles in the solar corona should be based on the modeling of all the parameters entering the formation process of these lines. This includes the coronal magnetic field, the solar wind outflow velocity, the density stratification of electrons and of atoms/ions, etc., at every point along the LOS. For the large scale magnetic field of the corona we adopt the model of Banaszkiewicz et al. (1998, see Fig. 1). The solar wind outflow speed is computed at any point of the solar corona using the mass-flux conservation equation which requires the knowledge of the electron density stratification. We consider a set of three different density stratifications all determined empirically by DKL, Guhathakurta & Holzer (1994, hereafter GH94) and Guhathakurta et al. (1999, hereafter Guh99) (see Fig. 2). The DKL density profile is obtained from SOHO observations (SUMER, UVCS and LASCO), while Guh99 densities are from LASCO and Mauna Loa observations and GH94 densities are from SKYLAB observations. Raouafi & Solanki (2004) have shown that the density stratification is a key quantity determining the off-limb profiles of collision-dominated lines, in particular the line width.

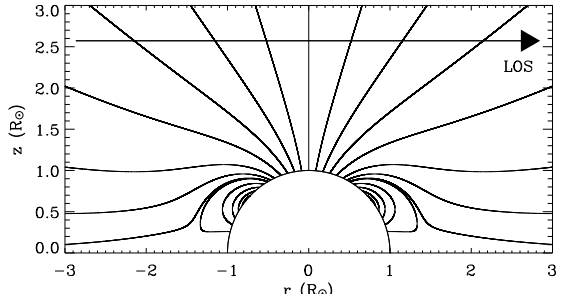


*Figure 1. Superradially expanding open magnetic field lines of the corona for the minimum of solar activity according to the model by Banaszkiewicz et al. (1998). A sample LOS is plotted through the northern coronal polar hole (horizontal arrow).*

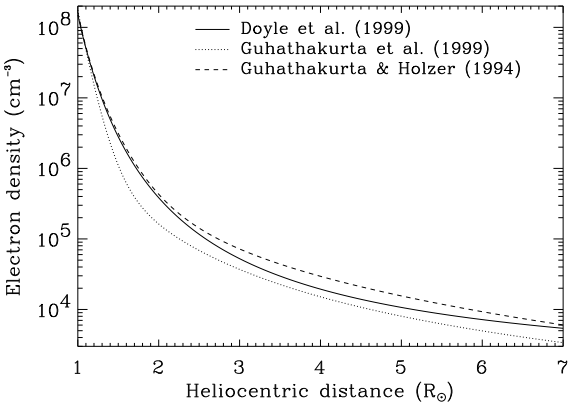


*Figure 2. Electron density plotted as a function of the distance to Sun center for different models (solid curve: DKL; dots: Guh99; dashes: GH94).*

The importance of the density profile resides therein that it influences the line profile integrated along the LOS directly through the total intensity, but also indirectly via the solar wind speed, which is determined via mass-flux

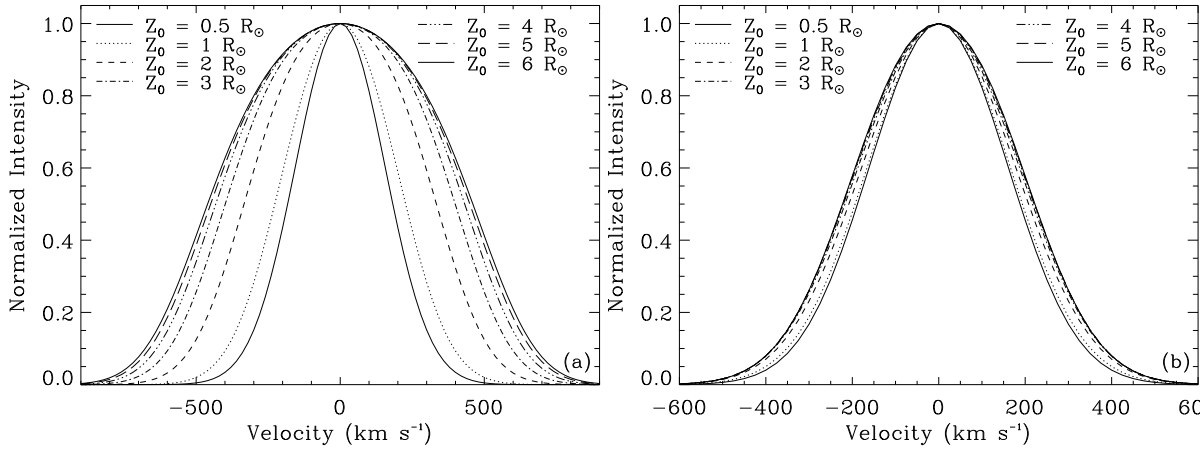


*Figure 3. Line profiles obtained by integrating over different distances between $-Z_0$ and $Z_0$ along the LOS for a spectral line excited only by electron collisions (a) and only by radiation (b). These profiles are obtained for a point of closest approach of $3.5\ R_\odot$ from Sun center and for $\alpha_s = 200$ km $s^{-1}$ ($\alpha_i = 100$ km $s^{-1}$ for the radiative component). The effect of the LOS integration on the radiatively excited lines is rather small compared to the case of collisional lines.*

conservation and thus depends on both the density stratification and the magnetic field. The stratification of emitting atoms/ions is very important as well, since it enters directly in both collisional and radiative components. Here we assume an atom/ion stratification identical to that of the electrons (for each density model).

## 4. EFFECT OF THE INTEGRATION ALONG THE LOS ON SPECTRAL PROFILES

In order to understand better the effect of the velocity field, density stratification and the integration along the LOS on the coronal lines, we study separately the effect of the LOS integration on the collisional and radiative components. This is useful for the interpretation of coronal observations, in particular for spectral lines that are composed of both components, such as the O VI doublet. The results presented in this section are obtained by using the electron density stratification of DKL (solid line in Fig. 2).

In Figure 3(a), the profiles of a pure collisional line obtained by integrating out to different distances along the LOS, $Z_0$, are displayed. For comparison in Figure 3(b) the profiles of a spectral line exclusively excited by radiation coming from the solar disk are plotted. These profiles are obtained for a projected heliocentric distance of $3.5\ R_\odot$. The different effect of the LOS integration on the profiles of each of the two types of lines is remarkable. The profile shape of the radiatively excited line is hardly altered by LOS integration, although the total intensity is significantly affected (not visible in Figure 3 due to the normalization). Profiles of pure collisional lines turn out to be sensitive to the atmospheric parameters out to surprisingly large $Z$ values along the LOS. In particular the widths of these lines are significantly affected by the large LOS velocities at large $|Z|$. Fig. 3 underlines the need to integrate out to $Z_0 = 6\ R_\odot$.

The electron density drops very fast at low altitudes ($< 2\ R_\odot$) and then the main contribution is given by the central part of the LOS (i.e. near the polar axis). However, when moving away from the solar disk, significant contributions are obtained from an increasingly larger section of the LOS, in particular to the line wings. For the collisional component this is due to the variation of the electron density as a function of the heliocentric distance. The density drops more slowly at larger altitudes (see Fig. 2) than at low altitudes. It is clear from Fig. 3 that the width of the collisionally dominated line profile is heavily affected by the LOS integration (due to the LOS component of the solar wind), while the profile of a radiatively excited line differs significantly less from the profile emitted by a unit volume just above the pole.

The behavior seen in Fig. 3 can be understood as follows. At a given $Z$, the Doppler shift of the collisional component is equal to the LOS speed $u_Z$ of the scattering atoms/ions (see first term of Eq. (1)). However, for the radiative component the Doppler shift is given by $(u_Z - \alpha_{si}\, n_Z\, \boldsymbol{u} \cdot \boldsymbol{n})$. Due to the supperradial expansion of the coronal magnetic field and to the increase of the solar wind outflow speed the Doppler shift of the collisional profiles increases when moving away from the point of closest approach to the solar surface along the LOS (i.e. moving to larger values of $|Z|$). That of the radiative component also increases at small $|Z|$, but ever more slowly at larger $|Z|$. Depending on the profile of the LOS velocity the line shift can reach a limiting value characteristic of that LOS (height above the solar limb), or can even start to decrease again at greater $|Z|$.

## 5. APPLICATION TO CORONAL LINES

Among the spectral lines observed by UVCS in polar coronal holes three sets are of particular interest. The first is the most intense line emitted in the solar corona,

H I Ly-$\alpha$ at 1215.62 Å. This line is emitted by the resonant scattering of the radiation emitted by the solar disk. The few electron collisions are negligible for this line (Raymond et al. 1997). The second group of lines is the O VI doublet at 1031.92 Å and 1037.61 Å. These lines are excited by both, the radiation coming from the underlying chromosphere-corona transition zone and by isotropic electron collisions. The third class is composed of the Mg X doublet at 609.793 Å and 624.941 Å, whose members are emitted following excitations produced almost exclusively by electron collisions in the solar corona.

### 5.1 The Ly-$\alpha$ line of hydrogen

To calculate the coronal emission, it is necessary to know the shape of the line profile coming from the solar disk (for the minimum of solar activity). The solar disk Ly-$\alpha$ has a complex shape (see Lemaire et al. 1998). A four Gaussian fit plus a constant background is applied to the solar disk Ly-$\alpha$ profile. We assume that coronal hydrogen atoms are illuminated by the photons of four incident Gaussian profiles emitted by the solar disk. We do not consider any limb-brightening or darkening for this line (see Bonnet et al. 1980).

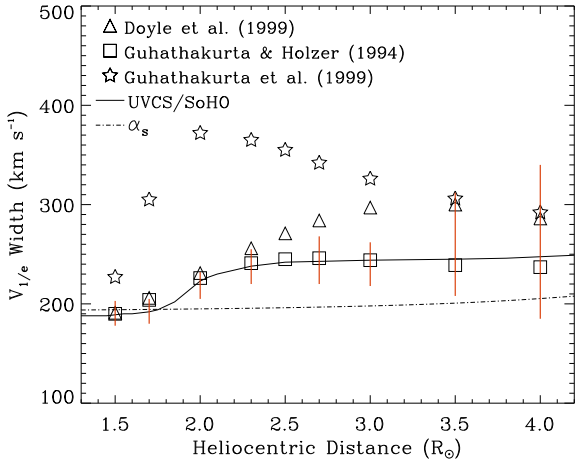


*Figure 4. Width of the LOS-integrated H I Ly-$\alpha$ line profile as a function of the projected heliocentric distance obtained for the different density stratification models presented in Fig. 2. The solid line is the best fit to the observations recorded by UVCS/SoHO and the dot-dashed line is the turbulence velocity distribution of the H I atoms. The vertical lines are the error bars of measured widths*

A single Gaussian is sufficient to fit the calculated off-limb Ly-$\alpha$ profiles. Fig. 4 displays the e-folding (Doppler) widths of the LOS integrated Ly-$\alpha$ profiles as a function of the projected heliocentric distance on the plane of the sky of each LOS. The values of $\alpha_s$ used to produce these profiles are also given in the same Figure (dot-dashed line) together with the best fit to the UVCS data (solid line) by Cranmer et al. (1999c) (see also Kohl et al. 1998). Clearly, the computed profiles are sensitive to the details of the electron density stratification. For the density stratification of GH94, the observed line width of H I Ly-$\alpha$ in polar coronal holes at different heights above the solar limb are comparable to the calculated ones in the presence of an isotropic velocity distribution and a gradual rise in $\alpha_s$ with heliocentric distance. The vertical lines are the 1-$\sigma$ error bars of UVCS measured widths (see Kohl et al. 1998; Cranmer et al. 1999; etc.). The stratification of DKL gives better results for a height independent $\alpha_s$.

### 5.2 O VI doublet

We compute the intensity profiles of the lines of the O VI doublet at 1031.92 Å and 1037.61 Å. In the solar corona, these lines are formed by electron collisions and by the scattering of the radiation coming from the transition region. We take into account the Doppler dimming due to the O VI ions' motion and the optical pumping of the O VI 1037.61 Å by the C II doublet (1036.33 Å, 1037 Å). All the solar disk line profiles are assumed to be Gaussians. We consider radiances of 305 and 152.5 and 52 erg cm$^{-2}$ s$^{-1}$ sr$^{-1}$ for the O VI 1031.92 Å and 1037.61 Å and the C II doublet, respectively. We assume also widths of 35 and 25 km s$^{-1}$ for the the O VI and C II doublets, respectively. We use the limb-brightening measured by Raouafi et al. (2002) for the O VI line and no limb-brightening for the C II lines (Warren et al. 1998).

The top panel of Fig. 5 displays the widths of the O VI 1031.92 Å line calculated for different projected heliocentric distances and for the three density models as a function of the heliocentric distance. These widths are obtained by applying a Gaussian fit to the calculated profiles. The dot-dashed curve gives the variation of the width $\alpha_S$ of the velocity distribution of the scattering ions. The solid line represents the best fit to the UVCS data (Cranmer et al. 1999c). Note that no anisotropy in the kinetic temperature of the emitting ions is considered.

At small heights (below 2 $R_\odot$) the widths of the calculated profile are comparable for all the density models except for the one by Guh99 where the density drops initially very rapidly compared to the two other models. This gives higher solar wind speeds and explains the broader profiles resulting from this model. All profiles are well represented by a Gaussian. At larger heights ($> 2.0\ R_\odot$) the line widths are very sensitive to the details of the electron density stratification. This can be easily seen by the difference in the width of the different profiles obtained through slightly different density stratification models. The model by Doyle et al. (solid line in Fig. 2) gives line widths comparable to the ones obtained from the data.

The bottom panel of Fig. 5 displays the ratio of total intensity of the O VI doublet lines ($\mathcal{I}_{1032}/\mathcal{I}_{1037}$) as a function of the projected heliocentric distance. This ratio exhibits a marked dependence on radial distance, being well over 2 close to the Sun, then dropping rapidly (except for the density models by Guh99, which produces a low ratio at small $r$). All the other models lead to a minimum in the ratio at $r = 2.3 - 2.7\ R_\odot$, which then increases again

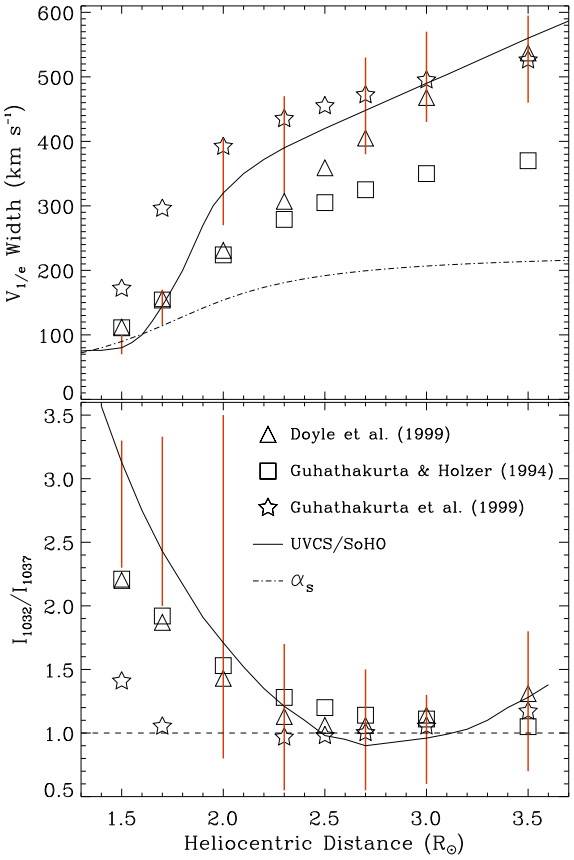


*Figure 5. Top panel: the symbols represent the variation of the width of the LOS integrated synthetic line profiles of O* VI *as a function of the heliocentric distance. The assignment of symbols to models is indicated in the bottom frame. The dot-dashed curve displays the used values of $\alpha_S$. The observed dependence is given by the solid curve. Bottom panel: the LOS integrated total intensity ratio of the O* VI *doublet lines ($\mathcal{I}_{1032}/\mathcal{I}_{1037}$) as a function of the heliocentric distance. The solid curve represents values deduced from observations performed by UVCS/SoHO and the vertical lines are the error bars of measured widths (see Cranmer et al. 1999).*

at larger $r$ (here the model of GH94 exhibits a slightly different behavior, showing a decrease in the ratio out to $r = 3.5\ R_\odot$). Generally, the ratios calculated from the Doyle et al. density model are close to the ones observed by UVCS/SoHO (vertical error bars).

### 5.3 Mg X doublet

The coronal Mg X ion emits a doublet at 609.793 Å and 624.941 Å that is formed in the solar corona almost exclusively by electron collisions. Due to the weakness of the polar coronal emission in these lines, UVCS/SoHO was only able to record data in the coronal polar holes up to a height of 2 $R_\odot$ from Sun center. The members of the doublet have almost identical widths, so that a single value suffices to describe both of them. The widths

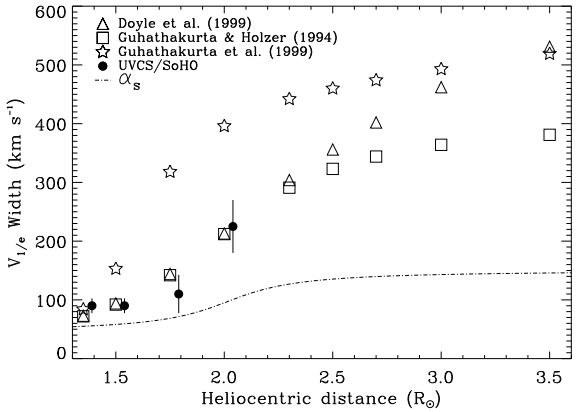


*Figure 6. Widths of the LOS integrated line profiles of the Mg* X *doublet plotted as a function of the projected heliocentric distance for the different density stratification models considered in the present paper. The dot-dashed line gives $\alpha_s$. Also plotted are the measured widths of the Mg* X *lines (full circles) together with the error bars (see Kohl et al. 1999). For the sake of clarity they are plotted slightly to the right from their respective x-coordinate values. The line profiles obtained at 3.5 $R_\odot$ for the different density models and those obtained by using Guh99 densities above 2.5 $R_\odot$ present a flattening at the central frequency which makes their one-Gaussian-fitting difficult.*

of the observed profiles are displayed in Fig. 6 together with their error bars (see Kohl et al. 1999). The widths of the calculated profiles and the values of microscopic velocities $\alpha_s$ used to reproduce these profiles are plotted in the same Figure. The obtained synthetic profile widths are comparable with the observed widths within the accuracy of the data. Note that we consider only the widths obtained from single Gaussian fits to the data, i.e. assuming no anisotropy of the velocity distribution.

## 6. DISCUSSION

We considered the influence of different density stratifications on line profiles with different formation processes (pure scattering lines, represented by H I Ly-$\alpha$; purely collisionally excited lines represented by the Mg X doublet, and line for which both process are important, represented by the O VI doublet). It is found that whereas the profile shape of the H I Ly-$\alpha$ line reacts less to the choice of density stratification, the width of the O VI and Mg X lines are strongly dependent. The line widths obtained and total intensity ratios of the O VI doublet at different heights in the polar coronal holes are found to be close to those obtained from observations carried out by SoHO/UVCS, in spite of the fact that we only consider an isotropic kinetic temperature of the scattering atoms and ions. We expect that with more refined models for the coronal densities, magnetic field and solar wind, the correspondence to the observations can be improved. These results have also an implication for the importance of anisotropy of kinetic temperature of the

heavy ions in the solar corona. Our analysis confirms the conclusion of Raouafi & Solanki (2004) that the need for anisotropic velocity distributions may not be so pressing as previously concluded. This in turn has implications for the mechanisms of heating and acceleration of different species in the polar coronal holes. We stress, however, that the current results do not rule out such anisotropies.

## ACKNOWLEDGMENTS

The authors would like to thank Steven Cranmer, Bernhard Fleck, Bernd Inhester, Eckart Marsch and Klaus Wilhelm for helpful discussions and critical comments that greatly improved the paper.

## REFERENCES

Bame, S. J., Asbridge, J. R., Feldman, W. C., Montgomery, M. D. and Gary, S. P. 1975, GRL, 2, 373

Banaszkiewicz M., Axford W. I. and McKenzie J. F. 1998, A&A, 337, 940

Bonnet, R. M., Decaudin, M., Bruner, E. C., Jr., Acton, L. W. and Brown, W. A 1980, ApJ, 237, L47

Collier, M. R., Hamilton, D. C., Gloeckler, G., Bochsler, P. and Sheldon, R. B. 1996, GeoRL, 23, 1191

Cranmer, S. R., Field, G. B. and Kohl, J. L. 1999a, ApJ, 518, 937

Cranmer, S. R., Field, G. B. and Kohl, J. L. 1999b, Space Sci. Rev., 87, 149

Cranmer, S. R., Kohl, J. L., Noci, G., et al. 1999c, ApJ, 511, 481

Domingo, V., Fleck, B. and Poland, A. I. 1995, Sol. Phys., 162, 1

Doyle, J. G., Keenan, F. P., Ryans, R. S. I., Aggarwal, K. M. and Fludra, A. 1999a, Sol. Phys., 188, 73

Doyle, J. G., Teriaca, L. and Banerjee, D. 1999b, A&A, 349, 956

Guhathakurta, M. and Holzer, T. E. 1994, ApJ, 426, 782

Guhathakurta, M., Fludra, A., Gibson, S. E., Biesecker, D. and Fisher, R. 1999, JGR, 104, 9801

Habbal, S. R., Woo, R., Fineschi, S., et al. 1997, ApJ, 489, L103

Hundhausen, A. J. 1972, *Coronal Expansion and Solar Wind*, Springer-Verlag, Berlin

Hyder, C. L. and Lites, B. W. 1970, Sol. Phys., 14, 147

Kohl, J. L. & Withbroe, G. L. 1982, ApJ, 256, 263

Kohl, J. L., Esser, R., Gardner, L. D., et al. 1995, Sol. Phys., 162, 313

Kohl, J. L., Noci, G., Antonucci, E., et al. 1997, Sol. Phys., 175, 613

Kohl, J. L., Noci, G., Antonucci, E., et al. 1998, ApJ, 501, L127

Lamy, P., Quemerais, E., Liebaria, A., et al. 1997, $5^{th}$ SoHO Workshop, ESA SP-404, p. 491

Lemaire, P., Emerich, C., Curdt, W., Schühle, U. and Wilhelm, K. 1998, A&A, 334, 1095L

Li, X., Habbal, S. R., Kohl, J. L. and Noci, G. 1998, ApJL, 501, L133

Marsch, E. 1999, Space Sci. Rev., 87, 1

Noci, G., Kohl, J. L. and Withbroe, G. L. 1987, ApJ, 315, 706

Noci, G., Kohl, J. L., Antonucci, E., et al. 1997, Adv. Space Res., 20, 2219

Raouafi, N.-E., Sahal-Bréchot, S., Lemaire, P., Bommier, V. 2002, A&A, 390, 691

Raouafi, N.-E. and Solanki, S. K. 2004, A&A, in press

Raymond, J. C., Kohl, J. L., Noci, G., et al. 1997, Sol. Phys., 175, 645

von Steiger, R., Geiss, J., Gloeckler, G. and Galvin, A. B. 1995, Space Sci. Rev., 72, 71

Warren, H. P., Mariska, J. T. and Wilhelm, K. 1998, ApJS, 119, 105